FEBS Letters 588 (2014) 3802–3807

journal homepage: www.FEBSLetters.org

Toll-like receptor 3 transmembrane domain is able to perform various homotypic interactions: An NMR structural study

Konstantin S. Mineev [a,*], Sergey A. Goncharuk [a,b], Alexander S. Arseniev [a]

[a] Shemyakin–Ovchinnikov Institute of Bioorganic Chemistry, Russian Academy of Sciences RAS, Str. Miklukho-Maklaya 16/10, Moscow 117997, Russian Federation
[b] Lomonosov Moscow State University, Moscow 119991, Russian Federation

ARTICLE INFO

Article history:
Received 24 June 2014
Revised 27 August 2014
Accepted 27 August 2014
Available online 12 September 2014

Edited by Christian Griesinger

Keyword:
Toll-like receptor
Transmembrane domain
Spatial structure
Dimerization
Free energy

ABSTRACT

Toll-like receptors (TLRs) take part in both the innate and adaptive immune systems. The role of the transmembrane domain in TLR signaling is still elusive, while its importance for the TLR activation was clearly demonstrated. In the present study the ability of the TLR3 transmembrane domain to form dimers and trimers in detergent micelles was shown by solution NMR spectroscopy. Spatial structures and free energy magnitudes were determined for the TLR3 transmembrane domain in dimeric and trimeric states, and two possible surfaces that may be used for the helix–helix interaction by the full-length TLR3 were revealed.

Structured summary of protein interactions:
TLR3-TM and **TLR3-TM** bind by nuclear magnetic resonance (1, 2)

1. Introduction

Toll-like receptors (TLRs) are one of the key players in both the innate and adaptive immune systems [1]. These proteins recognize pathogen-associated molecular patterns (PAMP), such as components of bacterial cell walls (human TLRs 1, 2, 4, 5, 6, 10) or viral nucleic acids (human TLRs 3, 7, 8, 9) and induce the release of the effector molecules of the immune system [2]. TLRs belong to the type I transmembrane proteins and consist of the extracellular ligand-binding domain extracellular domain (ECD), single transmembrane α-helix and intracellular Toll-interleukin I receptor domain (TIR), which is responsible for the downstream signaling [1,2]. According to crystal structures, TLRs form homo- or heterodimeric signaling complexes interacting with the single PAMP molecule [3–7]. The medical and biological significance of toll-like receptor (TLR) signaling is obvious, since the disregulation of the TLR system may cause various autoimmune diseases and septic shock [8–11], and some therapeutic strategies targeting TLRs have already emerged [8,11,12].

There is a lot of data available on the structural and biological aspects of the TLR signaling, mainly related to the roles of the (ECD) and TIR in the process. Moreover, a computer model of the dimeric full-length TLR3 receptor in the active state was build [4]. Nevertheless, the role of the transmembrane domain (TMD) in TLR signaling is still elusive, while its significance for the TLR activation was demonstrated in recent studies. In particular, it was shown that constitutively dimerizing ECDs can cause the ligand-independent activation of the receptor by bringing together isolated transmembrane domain (TMD) and TIR domains [13,14]. The TLR9 receptor was shown to exist as preformed dimers in the cell membrane, while ligand binding induces only the rearrangement of the subunits [15], which seems similar to the "coupled rotation" activation mechanism, implying the crucial role of the receptor TMD, proposed for some receptor tyrosine kinases [16]. And, last, it was demonstrated that decoupling of the ECD and TIR of TLR4 from the TMD can disrupt its signaling [17] and that TLR4 constructs with the deleted ECD are constitutively active and dimeric [18]. Isolated TMDs of all TLR receptors were shown to homodimerize in bacterial membranes, with TMDs of TLR2,3,8,9 having the highest propensity to perform homotypic interactions [19]. Taking into account all aforesaid, it is obvious that the structural investigations of TLR TMD dimers is necessary, because these domains can as well serve as targets for emerging therapies. In the present work the NMR study of homotypic interactions of TLR3 TMD is reported.

Abbreviations: TM, transmembrane; DPC, dodecylphosphocholine; TMD, isolated transmembrane domain; TLR, toll-like receptor; TFE, trifluoroethanol; TIR, Toll-interleukin I receptor domain; NOE, nuclear overhauser effect; NOESY, NOE spectroscopy; ECD, extracellular domain; PAMP, patogen-associated molecular patterns; FOS-16, hexadecylphosphocholine; LPR, lipid-to-protein ratio

* Corresponding author.
E-mail address: mineev@nmr.ru (K.S. Mineev).

http://dx.doi.org/10.1016/j.febslet.2014.08.031
0014-5793/

2. Materials and methods

2.1. Construction of expression plasmid

The gene encoding transmembrane and juxtamembrane residues 698–730 (MD[698]SAPFELFFMINTSILLIFIFIVLLIHFEGWRI, TLR3-TM) of human TLR3 was amplified by PCR from four chemically synthesized oligonucleotides (Evrogen, Russia) partially overlapped along their sequences. The PCR products were cloned into pET22b vector using ligation by NdeI and HindIII restriction sites. The final construct was confirmed by DNA sequencing.

2.2. Gene expression

The 34-residue TLR3-TM was expressed as precipitate of the reaction mixture (RM) in continuous exchange cell free (CF) expression system [20,21]. S30 CF extract from Rosetta(DE3)pLysS *E. coli* strain and T7 RNA polymerase were prepared by previously described protocol [22]. Optimal reaction conditions were performed using homemade reactors based on Mini-CECF-Reactor previously described [22] and membranes with molecular weight cut-off of 12.5 kDa. Preparative scale reactions (1–2 ml of RM) were carried out in 50 ml tubes. The optimal FM:RM ratio was 12:1 and RM contained 100 mM HEPES/0.83 mM EDTA/KOH at pH 8.0, 0.1 mg/mL folinic acid, 20 mM acetyl phosphate, 1.2 mM ATP and 0.8 mM each of G/C/UTP, 2 mM 1,4-dithiothreitol, 0.05% sodium azide, 2% PEG-8000, 20 mM magnesium acetate, 270 mM potassium acetate, 60 mM creatine phosphate, 1 mM each of 20 amino acid or 0.25% of 20 amino-acid mix (CIL), 1 tablet/50 mL complete protease inhibitor (Roche), 0.5 mg/mL *E. coli* tRNA (Roche), 0.25 mg/mL creatine kinase from rabbit muscle (Roche), 0.05 mg/mL T7 RNA polymerase, 0.1 U/mkL Ribolock (Fermentas), 0.02 mkg/mkL plasmid DNA, and 30% S30 CF extract. All reagents were provided by Sigma Aldrich, Germany unless otherwise specified. Reactions were conducted overnight at 30 °C and 150 rpm in an Innova 44R shaker (New Brunswick). 20-aminoacid mixture of 13C/15N-labeled amino acids (CIL) was used to obtain uniformly 13C/15N-labeled protein sample.

2.3. Protein purification and solubilization

The protein precipitate was washed three times by buffer containing 50 mM Tris pH 8.0 and 100 mM NaCl. RNAse A (Fermentas) with final concentration of 20 mkg/mkl was added into the buffer at first washing step. After each step protein was centrifuged for 10 min at 18 000 g at room temperature and supernatant aliquots were analyzed by 12,5% Tricine SDS–PAGE. The TLR3-TM was purified by dissolving the washed precipitate in TFE/H_2O mixture 2:1 and centrifuging for 10 min at 18 000×*g*. Dissolved protein was added to DPC-d38 (CIL) powder at the initial lipid-to-protein ratio (LPR) of 1:60. The concentration of TLR3-TM was assessed by the protein absorption at 280 nm and by 1D NMR spectroscopy in TFE/H_2O (with respect to the internal reference peak of 1 mM TSP). In order to achieve the incorporation of the peptide into the micelle particles the resulting solution was diluted with water to 1:1 TFE/H_2O ratio and lyophilized. Final NMR samples contained 0.9 mM of 13C/15N-TLR3-TM, 1.1 mM of 12C/14N-TLR3-TM, 120 mM of DPC-d38, 1 mM NaN3, and either 20 mM of sodium acetate at pH 4.5 or 20 mM of phosphate buffer at pH 7.5.

2.4. NMR spectroscopy

All NMR experiments were run on 600 and 800 MHz Avance III spectrometers equipped with cryogenic triple resonance probes (Bruker Biospin, Germany) at 45 °C. Free energies of dimerization and oligomerization of TLR3-TM were measured through the procedure described in [23]. Populations of the oligomeric states were determined from the intensities of 2D cross-peaks in BEST-TROSY spectra [24] acquired with the relaxation delay of 0.8 s (selective excitation T1 for amide protons was assessed as 0.15 s). Assignment of chemical shifts was performed via the standard approach [25] with use of triple resonance and NOE spectroscopy (NOESY) 3D NMR spectra. Non-uniform sampling in indirect dimensions [26] and BEST [27] pulse sequences were used to detect the triple resonance spectra. Constant-time evolution versions of NOESY-13C-HSQC and HCCH-TOCSY experiments [28] were used to assign signals from methyl groups of TLR3-TM. Spin-echo difference spectra were used to calculate vicinal J-couplings, depending on χ_1 dihedral angle [29,30]. 13C/15N-filtered-13C-edited-NOESY-HSQC [31] was recorded to directly detect intermolecular nuclear overhauser effect (NOE) connectivities. Backbone torsion angles restraints were obtained from the NMR chemical shifts in TALOS + software [32]. Spatial structures of dimer and trimer were calculated in CYANA 3.0 software [33], the obtained data were visualized in MOLMOL [34]software.

3. Results

3.1. TLR3 TMD can form stable dimers and trimers in dodecylphosphocholine (DPC) micelles

To study the homotypic interactions of TLR3 TMDs we have produced the peptide, corresponding to residues Asp[698]–Ile[730] of the full length receptor in the continuous exchange cell-free expression system. Assignment of NMR spectra acquired at lipid-to-protein ratio (LPR) 60 and pH 4.5 revealed that three sets of signals can be detected for both amide protons and methyl groups of TLR3-TM (Figs. 1A, B and S1). These sets are characterized by different correlation times for the rotational diffusion, indicating that signals correspond to different oilgomeric states (Fig. 1C). This was confirmed by dodecylphosphocholine (DPC) titration experiments – TLR3-TM appeared to form dimers and trimers, with standard free energy of dimerization and trimerization being equal to -1.8 ± 0.1 and -2.0 ± 0.1 kcal/M (at 1 M of detergent standard conditions) correspondingly (Fig. 1D and E). Therefore we can conclude that TLR3-TM forms dimers and trimers of moderate stability in DPC micelles, TLR3-TM dimer is more stable than the dimers of the TMDs of ErbB3 (−0.5 kcal/M, [35]), ErbB4 (−1.4 kcal/M, [36]) has comparable stability to FGFR3 (−2.8 to −1.4 kcal/M, [37,38]), but is much weaker than the dimers of glycophorin A (−7 to −5 kcal/M [39,40]) or VEGFR2 (−4.8 kcal/M, [23]) TMDs. Free energies of both dimerization and trimerization of the peptide were found to be dependent on ambient pH and hydrophobic thickness of the micelles, while the spatial structure of both dimers and trimers was retained, according to NMR chemical shift changes observed. Both types of helix–helix interactions were gradually destabilized by the increase of the pH in the range 4.0–7.5 by approximately 1 kcal/M (Fig. 1F). The pH dependence of the free energies correlated with the titration curve of both His[724] and Glu[726] sidechains of TLR3-TM (Fig. S2). On the other hand, addition of hexadecylphosphocholine (FOS-16) to DPC caused the gradual stabilization of both dimer and trimer up to ∼1 kcal/M at FOS-16/DPC ratio equal to 0.4 (Fig. S3).

3.2. Structural properties of TLR3-TM dimers and trimers

Despite the severe complexity of NMR spectra, containing three sets of signals, we managed to achieve almost 100% assignment of NMR resonances. To reveal the structural parameters of transmembrane helix–helix interactions of TLR3-TM peptide we used the

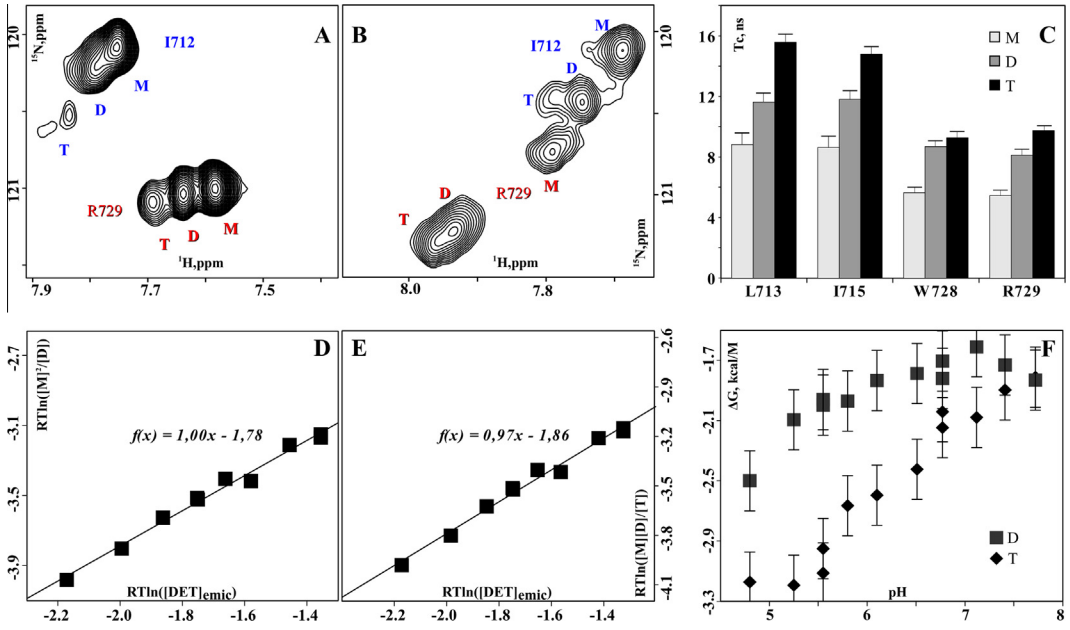

Fig. 1. (A,B) Fragments of 1H,15N-TROSY spectra of the TLR3-TM, containing cross-peaks from N–H groups of residues Ile^{712} and Arg^{729}. Spectra were acquired at pH 7.5 (A) or 4.5 (B) and LPR 80. (C) Correlation times of rotational diffusion measured for N–H groups of selected residues of TLR3-TM, in monomeric (M, light gray), dimeric (D, dark gray) and trimeric (T, black) states. Correlation times were calculated from cross-correlated NMR relaxation rates [46]. (D,E) Dependence of the apparent free energies of dimerization on the concentration of detergent in empty micelles at pH 7.5, used to determine the free energies of the dimerization (D) and trimerization (E) of the TLR3-TM. *R* is the universal gas constant, *T* is the temperature in K, [M], [D] and [T] are the concentration of monomers, dimers and trimers in solution, $[Det]_{emic}$ is the concentration of detergent in empty micelles. For details see [23]. Data were approximated by the linear dependence, results of the approximation are shown. (F) pH dependence of the standard free energies of dimerization (squares) and trimerization (rhomboids) of TLR3-TM.

heteronuclei-filtered NOESY NMR spectra [31], allowing direct detection of intermolecular distances between 13C/15N-labeled and unlabeled molecules (Fig. S7). Spectra were acquired at two conditions: at pH 4.5 and LPR 60, when monomer/dimer/trimer ratio was approximately 5/35/60 and at pH 7.5, LPR 120, when the ratio was 60/30/10 (Fig. S3). We intentionally selected conditions first with maximal contents of the trimeric form and then with maximal dimer/trimer ratio (to obtain the intermolecular NOEs, corresponding to the dimeric state only). Analysis of NOE contacts, observed in both spectra revealed that almost the whole surface of the transmembrane (TM) helix is used either for the dimerization or trimerization of the TLR3-TM (Fig. 2). Spectrum recorded at pH 7.5 had relatively poor sensitivity (due to the low concentration of dimeric species and extensive line broadening of some cross-peaks) and only three interhelical contacts were observed, between the sidechains of Thr^{710} and Leu^{714}. These contacts were then used to analyze the spectrum at pH 4.5, where the intensities of peaks corresponding to the trimeric and dimeric states were almost equal. The specified procedure allowed to determine three distinct contact surfaces, the one involved in the dimerization, including residues Phe^{706},Thr^{710}, Leu^{714} and Phe^{718}, and two others used for the trimerization, including residues Phe^{705}, Asn^{709},Leu^{713} and Ile^{717} on one side of the TM helix and Ile^{708}, Ile^{712} and Phe^{716} on the other. These data were used to determine the spatial structures of both dimer and trimer (Fig. 2B and C, Table S1). Unfortunately, NOE contacts to the sidechain of Asn^{13} were not observed, because its signals are extremely broad in NMR spectra, therefore the hydrogen bonding pattern, accomplished by its polar amide group is not determined.

In addition to the contact surfaces our data reveal that the secondary structure of the TLR3-TM is also affected by the dimerization/trimerization. According to the secondary chemical shifts of Cα nuclei, first two turns of the TM-helix (Phe^{702}–Asn^{709}) are destabilized for both monomeric and dimeric states in DPC, while this part of the TMD is quite stable for the trimeric state. This phenomenon is not observed in DPC/FOS-16 mixed micelles. Addition of FOS-16 to DPC gradually changes Cα chemical shifts of monomer until they almost exactly coincide with the chemical shifts of the trimeric state observed in pure DPC solution (Fig. S4). This observation is consistent with the fact that Asn^{709} is located on the trimerization interface. In monomeric and dimeric states Asn^{709} sidechain may tend to form intramolecular hydrogen bonds, which may cause the destabilization of the TM helix.

NMR chemical shifts and solved spatial structures were deposited to BMRB and PDB with accession codes 19674, 2mk9 and 2mka.

4. Discussion

One of the reasons why we selected TLR3 for the current study is the peculiar aminoacid sequence of its TMD. It includes unusually large quantity of aromatic residues – 6 Phe and Trp and a cluster of relatively polar residues (Asn^{709}Thr^{710}Ser^{711}) deep inside the membrane. It is well-known that highly polar residues in TM helices can drive their association [41,42], and slightly polar residues, such as Gly, Ser, Thr and Ala can mediate the TM helix–helix interactions if they are put together in special motifs, such as GxxxG or "heptad-repeat" [43,44]. Aromatic sidechains also bear partial charges and can engage in electrostatic interactions with other aromatic residues or polar sidechains, thus stabilizing the dimerization/oligomerization of TM segments [45]. Nevertheless, none of the putative helix interaction motifs are found in the sequence of TLR3-TM. In this respect, it is rather interesting to analyze the obtained structures. Here we report the ability of TLR3-TM to form dimers and trimers with different surfaces for helix–helix interaction. While the dimeric structure is stabilized by the van-der-Waals interactions between bulky sidechains and stacking of aromatic rings of Phe^{706} and Phe^{718}, the trimer formation is supported by the contacts between polar sidechains of Asn^{709}, stacking of Phe^{705} and Phe^{716} aromatic rings and by the van-der-Waals

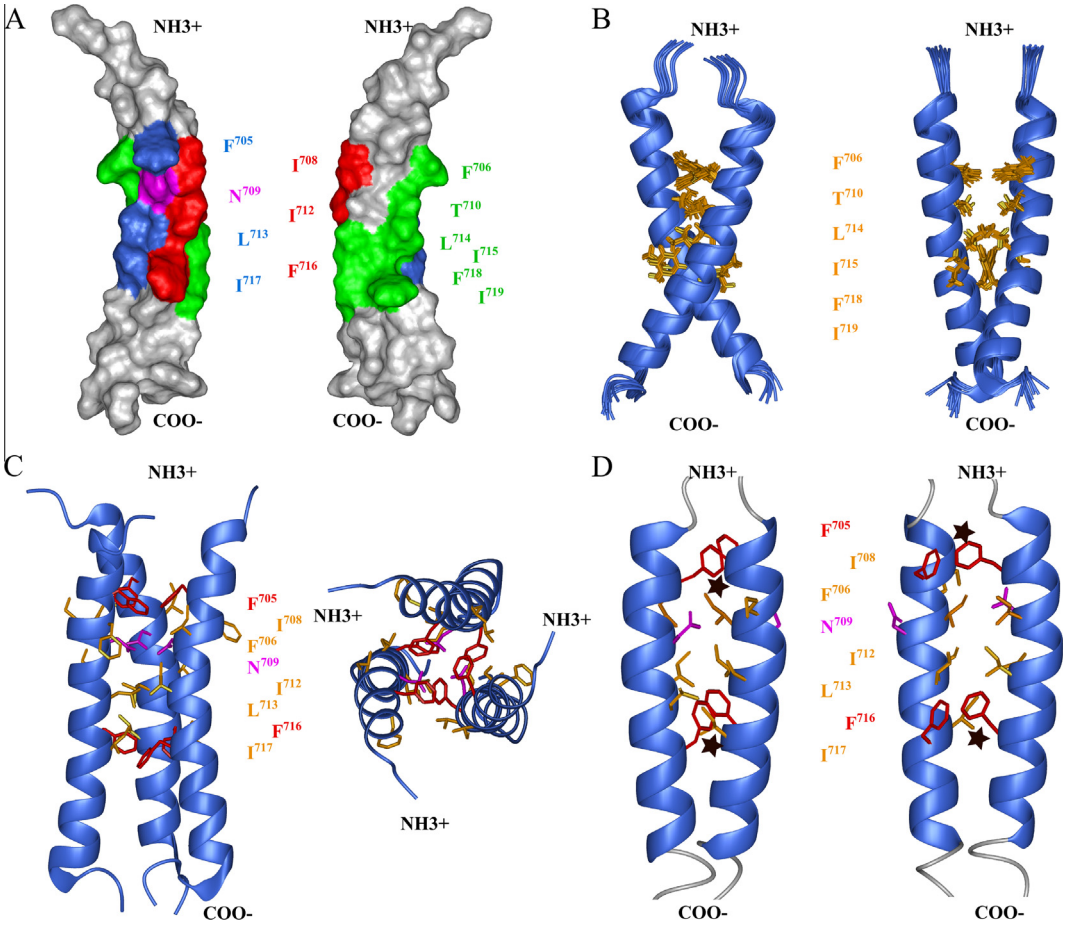

Fig. 2. (A) Molecular surface of TLR3-TM is painted with respect of observed NOE connectivities. Residues with detected intermolecular NOE's in the dimer/trimer 1:2 mixture are divided into three surfaces: dimerization interface (green) and two surfaces employed for the trimerization (blue and green). Asn^{709} is shown in magenta. (B) Set of 20 best calculated spatial structures of TLR3-TM dimer in ribbon representation. Sidechains of residues on the dimerization interface are shown by cylinders. (C) Determined spatial structure of TLR3-TM in ribbon representation. Sidechains of residues on the dimerization interface are shown by cylinders. Phe^{705} and Phe^{716} sidechains are shown in red, Asn^{709} sidechain is shown in magenta. (D) Asymmetric structure of the dimeric TMD of the TLR3, as predicted by the model of the full-length receptor [4]. Sidechain color code is the same as on panel (C). Places of steric hindrances are highlighted by black stars.

contacts between branched and non-polar residues. In addition, Thr^{710} lies on the dimerization interface, but its sidechain does not take part in any polar intermolecular contacts, instead forming the intramolecular hydrogen bond with carbonyl group of Phe^{706} and another polar contact with the partial charge on its aromatic ring. Therefore we can conclude that dimerization is driven mainly by aromatic sidechains, while both aromatic residues and a polar cluster play role in trimerization of TLR3-TM.

One may argue that the trimeric structure seems irrelevant form the biological point, since the full-length TLR3 receptor never forms trimers, but it uncovers the alternative way of helix–helix interaction inside the dimeric TMD of the TLR3. In the symmetric trimer each helix has two interaction surfaces and pairwise interactions between α-helices is asymmetric. In this respect the spatial structure of TLR3-TM trimer provides the information on the interface of possible asymmetric dimerization of the TLR3 TMDs. This interface is characterized by substantially higher free energy, because no dimer, employing the found surfaces is observed, but still it can be brought into effect in the full-length receptor.

The biological relevance of the contact surfaces determined for the trimeric structure of TLR3-TM is supported by the model of the full-length TLR3 receptor in the active state, constructed on the basis of crystal structures of dimeric ECD and TIR domain in the group of prof. Davies [4]. In this model TM helix has the same disposition as was found in the present work – it starts at Phe^{702} and ends at Phe^{725}. Moreover, the structure of the dimeric TMD is asymmetric and Asn^{709} is located on the dimerization interface of one TM helix, while it is located aside from the contact area of the second helix (Fig. 2D). Additionally, Ile^{712}, Leu^{713}, Ile^{715}, Phe^{716} and Ile^{717} are on the dimerization interface, which is similar to determined in the present work trimeric structure. On the other hand the structural parameters of helix–helix interaction in the full-length model are different from the reported for the TLR3-TM trimer. Transmembrane helices are slightly rotated and are located closer in the full-length TLR3 model and the helix-helix interface is extended towards the C-terminus of the TM domain. However, we need to note, that the discussed model suffers from the steric clashes in the TM region, and in reality the interaction of TLR3 TMDs has to be slightly different and even may fit to the experimentally determined parameters of the reported trimeric structure of the TLR3-TM. Therefore, we can state that the parameters of TM helix–helix interactions, observed in the trimeric structure of the TLR3-TM are close to the ones obtained in the full-size model of the dimeric TLR3 receptor, and the observed trimeric structure is likely to be relevant from the biological point. The helix–helix interaction interface obtained in the present study for the TLR3-TM dimer may also be employed by the full-size receptor if the inactive dimeric state of the TLR3 is possible.

In summary, the structural and energetic parameters of helix–helix interactions accomplished by TLR3 TMDs are reported. We

show that TLR3-TM can form moderately stable dimers and trimers in detergent micelles, with stability of associates being dependent on ambient pH and hydrophobic thickness of membrane mimetic. NMR data revealed two possible surfaces that may be used for the transmembrane helix–helix interaction. The obtained data provides an insight into the "blind spot" of TLR3 signaling – structure of the transmembrane domain in the dimeric state, and can be used in further mutagenesis studies, which are necessary to elucidate the role of transmembrane domains in the processes of signal transduction by the TLR3 receptor.

Acknowledgments

The work was supported by the Russian Scientific Foundation (Grant #14-14-00573). Authors acknowledge the group of professor David Davies, NIH, for the coordinates of the molecular model of the full-length TLR3.

Appendix A. Supplementary data

Supplementary data associated with this article can be found, in the online version, at http://dx.doi.org/10.1016/j.febslet.2014.08.031.

References

[1] Medzhitov, R. (2001) Toll-like receptors and innate immunity. Nat. Rev. Immunol. 1, 135–145, http://dx.doi.org/10.1038/35100529.
[2] Kawai, T. and Akira, S. (2010) The role of pattern-recognition receptors in innate immunity: update on Toll-like receptors. Nat. Immunol. 11, 373–384, http://dx.doi.org/10.1038/ni.1863.
[3] Leonard, J.N., Ghirlando, R., Askins, J., Bell, J.K., Margulies, D.H., Davies, D.R., et al. (2008) The TLR3 signaling complex forms by cooperative receptor dimerization. Proc. Natl. Acad. Sci. U.S.A. 105, 258–263, http://dx.doi.org/10.1073/pnas.0710779105.
[4] Liu, L., Botos, I., Wang, Y., Leonard, J.N., Shiloach, J., Segal, D.M., et al. (2008) Structural basis of Toll-like receptor 3 signaling with double-stranded RNA. Science 320, 379–381, http://dx.doi.org/10.1126/science.1155406.
[5] Jin, M.S., Kim, S.E., Heo, J.Y., Lee, M.E., Kim, H.M., Paik, S.-G., et al. (2007) Crystal structure of the TLR1–TLR2 heterodimer induced by binding of a tri-acylated lipopeptide. Cell 130, 1071–1082, http://dx.doi.org/10.1016/j.cell.2007.09.008.
[6] Kang, J.Y., Nan, X., Jin, M.S., Youn, S.-J., Ryu, Y.H., Mah, S., et al. (2009) Recognition of lipopeptide patterns by Toll-like receptor 2-Toll-like receptor 6 heterodimer. Immunity 31, 873–884, http://dx.doi.org/10.1016/j.immuni.2009.09.018.
[7] Park, B.S., Song, D.H., Kim, H.M., Choi, B.-S., Lee, H. and Lee, J.-O. (2009) The structural basis of lipopolysaccharide recognition by the TLR4-MD-2 complex. Nature 458, 1191–1195, http://dx.doi.org/10.1038/nature07830.
[8] Cook, D.N., Pisetsky, D.S. and Schwartz, D.A. (2004) Toll-like receptors in the pathogenesis of human disease. Nat. Immunol. 5, 975–979, http://dx.doi.org/10.1038/ni1116.
[9] Goh, F.G. and Midwood, K.S. (2012) Intrinsic danger: activation of Toll-like receptors in rheumatoid arthritis. Rheumatol. Oxford Engl. 51, 7–23, http://dx.doi.org/10.1093/rheumatology/ker257.
[10] Montero Vega, M.T. and De Andrés Martín, A. (2009) The significance of toll-like receptors in human diseases. in: Allergol. Immunopathol. (Madr.) 37, 252–263, http://dx.doi.org/10.1016/j.aller.2009.04.004.
[11] O'Neill, L.A.J., Bryant, C.E. and Doyle, S.L. (2009) Therapeutic targeting of Toll-like receptors for infectious and inflammatory diseases and cancer. Pharmacol. Rev. 61, 177–197, http://dx.doi.org/10.1124/pr.109.001073.
[12] Krishnan, J., Lee, G. and Choi, S. (2009) Drugs targeting Toll-like receptors. Arch. Pharmacal Res. 32, 1485–1502, http://dx.doi.org/10.1007/s12272-009-2100-6.
[13] Hasan, U.A., Dollet, S. and Vlach, J. (2004) Differential induction of gene promoter constructs by constitutively active human TLRs. Biochem. Biophys. Res. Commun. 321, 124–131, http://dx.doi.org/10.1016/j.bbrc.2004.06.134.
[14] Zhang, H., Tay, P.N., Cao, W., Li, W. and Lu, J. (2002) Integrin-nucleated Toll-like receptor (TLR) dimerization reveals subcellular targeting of TLRs and distinct mechanisms of TLR4 activation and signaling. FEBS Lett. 532, 171–176.
[15] Latz, E., Verma, A., Visintin, A., Gong, M., Sirois, C.M., Klein, D.C.G., et al. (2007) Ligand-induced conformational changes allosterically activate Toll-like receptor 9. Nat. Immunol. 8, 772–779, http://dx.doi.org/10.1038/ni1479.
[16] Moriki, T., Maruyama, H. and Maruyama, I.N. (2001) Activation of preformed EGF receptor dimers by ligand-induced rotation of the transmembrane domain. J. Mol. Biol. 311, 1011–1026, http://dx.doi.org/10.1006/jmbi.2001.4923.
[17] Treeby, M., Vasl, J., Ota, P., Friedrich, J. and Jerala, R. (2009) Different functional role of domain boundaries of Toll-like receptor 4. Biochem. Biophys. Res. Commun. 381, 65–69, http://dx.doi.org/10.1016/j.bbrc.2009.02.017.
[18] Panter, G. and Jerala, R. (2011) The ectodomain of the Toll-like receptor 4 prevents constitutive receptor activation. J. Biol. Chem. 286, 23334–23344, http://dx.doi.org/10.1074/jbc.M110.205419.
[19] Godfroy, J.I., Roostan, M., Moroz, Y.S., Korendovych, I.V. and Yin, H. (2012) Isolated Toll-like receptor transmembrane domains are capable of oligomerization. PLoS One 7, e48875, http://dx.doi.org/10.1371/journal.pone.0048875.
[20] Schwarz, D., Junge, F., Durst, F., Frölich, N., Schneider, B., Reckel, S., et al. (2007) Preparative scale expression of membrane proteins in Escherichia coli-based continuous exchange cell-free systems. Nat. Protoc. 2, 2945–2957, http://dx.doi.org/10.1038/nprot.2007.426.
[21] Spirin, A.S., Baranov, V.I., Ryabova, L.A., Ovodov, S.Y. and Alakhov, Y.B. (1988) A continuous cell-free translation system capable of producing polypeptides in high yield. Science 242, 1162–1164.
[22] Kai, L., Roos, C., Haberstock, S., Proverbio, D., Ma, Y., Junge, F., et al. (2012) Systems for the cell-free synthesis of proteins. Methods Mol. Biol. Clifton NJ. 800, 201–225, http://dx.doi.org/10.1007/978-1-61779-349-3_14.
[23] Mineev, K.S., Lesovoy, D.M., Usmanova, D.R., Goncharuk, S.A., Shulepko, M.A., Lyukmanova, E.N., et al. (2014) NMR-based approach to measure the free energy of transmembrane helix–helix interactions. Biochim. Biophys. Acta 1838, 164–172, http://dx.doi.org/10.1016/j.bbamem.2013.08.021.
[24] Favier, A. and Brutscher, B. (2011) Recovering lost magnetization: polarization enhancement in biomolecular NMR. J. Biomol. NMR 49, 9–15, http://dx.doi.org/10.1007/s10858-010-9461-5.
[25] Cavanagh, J. (2007) Protein NMR Spectroscopy: Principles and Practice, second ed, Academic Press, Amsterdam, Boston.
[26] Orekhov, V.Y. and Jaravine, V.A. (2011) Analysis of non-uniformly sampled spectra with multi-dimensional decomposition. Prog. Nucl. Magn. Reson. Spectrosc. 59, 271–292, http://dx.doi.org/10.1016/j.pnmrs.2011.02.002.
[27] Schanda, P., Van Melckebeke, H. and Brutscher, B. (2006) Speeding up three-dimensional protein NMR experiments to a few minutes. J. Am. Chem. Soc. 128, 9042–9043, http://dx.doi.org/10.1021/ja062025p.
[28] Uhrìn, D., Uhrínová, S., Leadbeater, C., Nairn, J., Price, N.C. and Barlow, P.N. (2000) 3D HCCH3-TOCSY for resonance assignment of methyl-containing side chains in 13C-labeled proteins. in: J. Magn. Reson. 142, 288–293, http://dx.doi.org/10.1006/jmre.1999.1951.
[29] Grzesiek, S., Vuister, G.W. and Bax, A. (1993) A simple and sensitive experiment for measurement of JCC couplings between backbone carbonyl and methyl carbons in isotopically enriched proteins. J. Biomol. NMR 3, 487–493.
[30] Vuister, G.W., Wang, A.C. and Bax, A. (1993) Measurement of three-bond nitrogen-carbon J couplings in proteins uniformly enriched in nitrogen-15 and carbon-13. J. Am. Chem. Soc. 115, 5334–5335.
[31] Zwahlen, C., Legault, P., Vincent, S.J.F., Greenblatt, J., Konrat, R. and Kay, L.E. (1997) Methods for measurement of intermolecular NOEs by multinuclear NMR spectroscopy: application to a bacteriophage λ N-peptide/boxB RNA complex. J. Am. Chem. Soc. 119, 6711–6721, http://dx.doi.org/10.1021/ja970224q.
[32] Shen, Y., Delaglio, F., Cornilescu, G. and Bax, A. (2009) TALOS+: a hybrid method for predicting protein backbone torsion angles from NMR chemical shifts. J. Biomol. NMR 44, 213–223, http://dx.doi.org/10.1007/s10858-009-9333-z.
[33] Güntert, P., Mumenthaler, C. and Wüthrich, K. (1997) Torsion angle dynamics for NMR structure calculation with the new program DYANA. J. Mol. Biol. 273, 283–298, http://dx.doi.org/10.1006/jmbi.1997.1284.
[34] Koradi, R., Billeter, M. and Wüthrich, K. (1996) MOLMOL: a program for display and analysis of macromolecular structures. J. Mol. Graph. 14 (51–55), 29–32.
[35] Mineev, K.S., Khabibullina, N.F., Lyukmanova, E.N., Dolgikh, D.A., Kirpichnikov, M.P. and Arseniev, A.S. (1808) Spatial structure and dimer–monomer equilibrium of the ErbB3 transmembrane domain in DPC micelles. Biochim. Biophys. Acta 2011, 2081–2088, http://dx.doi.org/10.1016/j.bbamem.2011.04.017.
[36] Bocharov, E.V., Mineev, K.S., Goncharuk, M.V. and Arseniev, A.S. (1818) Structural and thermodynamic insight into the process of "weak" dimerization of the ErbB4 transmembrane domain by solution NMR. Biochim. Biophys. Acta 2012, 2158–2170, http://dx.doi.org/10.1016/j.bbamem.2012.05.001.
[37] Bocharov, E.V., Lesovoy, D.M., Goncharuk, S.A., Goncharuk, M.V., Hristova, K. and Arseniev, A.S. (2013) Structure of FGFR3 transmembrane domain dimer: implications for signaling and human pathologies. Struct. Lond. Engl. 1993 (21), 2087–2093, http://dx.doi.org/10.1016/j.str.2013.08.026.
[38] Merzlyakov, M., Chen, L. and Hristova, K. (2007) Studies of receptor tyrosine kinase transmembrane domain interactions: the EmEx-FRET method. J. Membr. Biol. 215, 93–103, http://dx.doi.org/10.1007/s00232-007-9009-0.
[39] Fisher, L.E., Engelman, D.M. and Sturgis, J.N. (1999) Detergents modulate dimerization, but not helicity, of the glycophorin A transmembrane domain. J. Mol. Biol. 293, 639–651, http://dx.doi.org/10.1006/jmbi.1999.3126.
[40] Fleming, K.G. (2002) Standardizing the free energy change of transmembrane helix–helix interactions. J. Mol. Biol. 323, 563–571, http://dx.doi.org/10.1016/S0022-2836(02)00920-8.
[41] Choma, C., Gratkowski, H., Lear, J.D. and DeGrado, W.F. (2000) Asparagine-mediated self-association of a model transmembrane helix. Nat. Struct. Biol. 7, 161–166, http://dx.doi.org/10.1038/72440.
[42] Zhou, F.X., Cocco, M.J., Russ, W.P., Brunger, A.T. and Engelman, D.M. (2000) Interhelical hydrogen bonding drives strong interactions in membrane proteins. Nat. Struct. Biol. 7, 154–160, http://dx.doi.org/10.1038/72430.

[43] Russ, W.P. and Engelman, D.M. (2000) The GxxxG motif: a framework for transmembrane helix–helix association. J. Mol. Biol. 296, 911–919, http://dx.doi.org/10.1006/jmbi.1999.3489.
[44] Walters, R.F.S. and DeGrado, W.F. (2006) Helix-packing motifs in membrane proteins. Proc. Natl. Acad. Sci. 103, 13658–13663, http://dx.doi.org/10.1073/pnas.0605878103.
[45] Sal-Man, N., Gerber, D., Bloch, I. and Shai, Y. (2007) Specificity in transmembrane helix–helix interactions mediated by aromatic residues. J. Biol. Chem. 282, 19753–19761, http://dx.doi.org/10.1074/jbc.M610368200.
[46] Chill, J.H., Louis, J.M., Baber, J.L. and Bax, A. (2006) Measurement of 15N relaxation in the detergent-solubilized tetrameric KcsA potassium channel. J. Biomol. NMR 36, 123–136, http://dx.doi.org/10.1007/s10858-006-9071-4.